A Novel Design Approach for Low-Speed Recovery of High-Performance Fighter Aircrafts

S.K. Jebakumar,[#] Abhay Pashilkar[$,*] and N. Sundararajan[%]

[#]*Academy of Scientific and Innovative Research (AcSIR), Ghaziabad - 201 002, India*
[$]*Systems Engineering Division, CSIR - National Aerospace Laboratories, Bengaluru – 560 017, India*
[%]*Electrical Engineering Dept., Nanyang Technological University, Singapore*
[*]*E-mail: apash@nal.res.in*

ABSTRACT

In this paper, a novel design approach for low-speed recovery of a high-performance fighter aircraft is presented. It is shown that the phugoid mode has an important bearing on the problem of low-speed departure. Based on the analysis of the phugoid mode trajectories, a novel low-speed protection algorithm is presented in this paper. The proposed low speed recovery is achieved in three phases. The first phase consists of detecting the incipient departure followed in the second phase by the application of suitable recovery controls and finally the third phase ends with the transfer of controls to the pilot. The design of the first and the third phase consist of choosing the correct trigger conditions which ensures safe recovery of the aircraft in all conditions. The proposed automatic low speed recovery is triggered when the aircraft trajectory crosses a fixed boundary in the region spanned by the dynamic pressure and its rate of decrease. It is observed that this boundary is approximately a straight line, implying that it is equivalent to a forward prediction in time to indicate when the aircraft will reach the lowest controllable airspeed. This Automatic Low Speed Recovery with Forward Prediction (ALSR-FP) algorithm is found to be simpler than other existing design methods and effective in preventing low speed departure for a variety of pilot inputs that result in the aircraft losing airspeed leading to stall. In the second phase control inputs are chosen to align the velocity vector to the direction of local gravity. The recovery phase is considered complete after the aircraft reaches the dynamic pressure which is approximately 10 % higher than the minimum dynamic pressure for control. Performance of the ALSR-FP is demonstrated using the high-performance fighter aircraft Aero-Data Model In a Research Environment (ADMIRE) model which has a delta wing configuration, canards and multiple redundant controls. It is also shown that the proposed algorithm can be easily implemented on board for any other fighter and civil aircraft.

Keywords: Low-speed recovery; Automatic flight control; High performance fighter aircraft

NOMENCLATURE

U,V,W	Aircraft velocity in body axis
P,Q,R	Aircraft angular velocity in body axis
ϕ,θ	Roll and pitch angles
F_x, F_y, F_z	Net aerodynamic force in body axis (x,y,z) respectively
T	Aircraft thrust
m	Mass of aircraft
g	Acceleration due to gravity
'α'	Angle of attack
'β'	Angle of sideslip
'γ'	Flight path angle
'τ'	Command path filter time constant
C_L, C_D	Lift and drag coefficients respectively
Vdot, γdot	Derivative of V and γ respectively

Units

1 Knot = 0.5144 m/s

1. INTRODUCTION

A good review of the history of aircraft Flight Control System (FCS) development from its early years till the present day has been presented by Abzug & Larrabee[1]. This development spans the initial mechanical control systems consisting of cable and push-pull rods to modern stability augmentation systems which are designed to provide adequate aircraft flying qualities. Modern FCS meets the demands of high-performance aircraft in terms of manoeuvrability and agility while respecting flight parameter limits on response variables like angle of attack, normal acceleration, lateral acceleration as well as control surface actuator position and rate limits. Typically, such aircrafts are open loop unstable.

Modern digital fly-by-wire control systems are capable of controlling highly unstable aircrafts with their times to double amplitude of the order of 180 ms[1]. This technology has been used to expand the operating ranges of aircraft's flight envelope and has permitted aircraft to fly in highly non-linear flow regimes[2-5]. A flight control system designed by local linearization performs well in linear regions and degrades significantly in the non-linear flow regimes where higher angles of attack and angular rates are present. Non-linear flight controller design technology like Nonlinear Dynamic Inversion (NDI) design has been

developed to control the aircraft in those regions where the effects of kinematic coupling, inertial coupling and gravity terms dominate[6-7]. Recently, further simplifications have been made in the NDI design referred to as Simplified Nonlinear Dynamic Inversion (SNDI) control design methodology in[8] leading a shorter design cycle time.

Carefree manoeuvring capability of an aircraft is a critical aspect of flight controller design of a modern fighter aircraft. Carefree manoeuvring is defined as the ability of flight control laws of a fighter aircraft to protect against its departure into an uncontrolled flight regime for any possible combinations of pilot inputs while at the same maintaining its performance. Hence, the first step in achieving carefree manoeuvring is to determine these regimes of flight where the aircraft is controllable (operating envelope) and where it is uncontrollable (also called as critical regimes) or the regimes where it exhibits un-commanded motions. Critical flight regimes usually involve higher angles of attack, higher rates of rotation or both[9]. Typical critical flight regimes of a fighter aircraft are shown in Fig. 1.
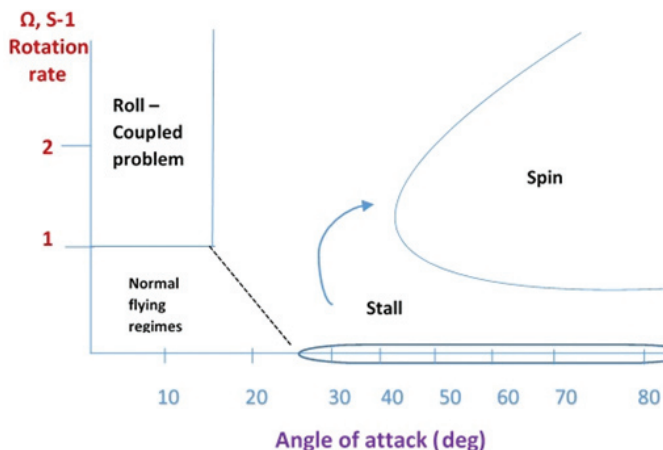

Figure 1. Critical regimes of flight.[9]

Every modern fighter aircraft has carefree manoeuvring capability built into its flight control system in view of benefits like improved mission effectiveness and performance. On the other hand, the difficulties in designing carefree manoeuvring capability are system complexity and the need for intensive test efforts to achieve this. A detailed discussion on the above aspects can be found in RTO TR-29[10].

In early carefree controller designs, the envelope restriction was implemented in a passive manner, where only a warning is provided to the pilot and the pilot has to take necessary actions for the recovery[10].The recovery will fail if the pilot does not notice a critical parameter like airspeed, attitude etc. or if he is temporarily in an unconscious state and cannot react. Subsequently, design improvements were made to provide an active carefree capability, where the aircraft operating parameters were limited automatically without pilot intervention. In this active scheme, the flight control system imposes the needed limits automatically. The aircraft state variables are prevented from exceeding their critical limits by the use of limiters in the inner loops of the FCS[11]. The departure in the lateral / directional path could occur due to the exceedance of 'β'. The proper design of Aileron Rudder Interconnect prevents the exceedance of aircraft parameters and departure[12].

From the available statistics of fighter aircraft accidents, one can see that many of the accidents are due to the exceedance of their low-speed limits and hence subsequent departures. In the modern fighter aircraft, the pilot is equipped with advanced flight controls and cockpit display, etc, to accomplish the multiple tasks in a mission. Hence a carefree manoeuvring capability becomes a mandatory requirement for a modern fighter aircraft. The Automatic Low Speed Recovery (ALSR) is an automatic recovery algorithm implemented in the modern flight control system to achieve the carefree manoeuvring capability. Based on the available literature, two low speed recovery techniques have been used earlier in contemporary aircraft programs. One is a Pilot Activated Recovery System (PARS) in a highly modified single seater fighter aircraft of USAF[10] and the other one is a sophisticated ALSR for the Eurofighter aircraft[13].

For the USAF aircraft, different recovery techniques were proposed at different regions based on the pitch attitudes of the aircraft as shown in Fig. 2. It can be seen that when the aircraft pitch attitude is high (greater than 70º), the suggested recovery technique is to execute a '5 g Pull through'.

For the Eurofighter aircraft, different recovery techniques were implemented based on the 'γ' under different ranges[13]. When 'γ'<40º, the recovery is done by pushing the pitch stick forward; when 'γ' is between 40º and 70º, the recovery is by a Knife over manoeuvre with pull input and for the condition of flight path angle greater than 70 º, the inverted pull is used for recovery. The Eurofighter ALSR low speed trigger is a function of γ, Vdot, γdot, mass, throttle, configuration, etc. It may be noted that both the approaches attempt to align the aircraft flight path in the direction of the gravity vector as quickly as possible. However, it may be noted that the design details of both these approaches are not available in the public domain for one to make a detailed analysis.

In this paper, starting from first principles, we present a simple and novel Auto Low Speed Recovery method with Forward Prediction (ALSR-FP) of the departure condition for a high-performance fighter aircraft. The method is based on a detailed study of the phugoid mode of the aircraft which deals with the interaction between the kinetic to potential energies as a function of time. The dynamic pressure is an indication of the kinetic energy of the aircraft. Aerodynamic control effectiveness is reduced at low speeds and hence at low dynamic pressures. The novel approach proposed in this paper is based on triggering an automatic recovery that is activated on entering a no-go region in a region spanned by dynamic pressure and its rate of decrease. Once the recovery is triggered, the pilot inputs are disregarded and the system goes into an automatic recovery mode. If the aircraft bank angle is below 60º, the aircraft angle of attack is driven to zero and the bank angle is brought to zero. On the other hand, if the bank angle is more than 60º, the aircraft is made to execute an inverted pull-down manoeuvre. These manoeuvres are designed to align the aircraft's velocity vector to the gravity vector. Once the airspeed recovers above a safe threshold, the controls are handed over back to the pilot.

Simulations with different types of pilot inputs that result in a decay of airspeed have been used for testing the recovery algorithm. ALSR-FPhas been shown to protect the aircraft from the violation of its minimum speed limit and the subsequent

departure across the whole ranges of Mach numbers and altitudes. Our approach to low-speed recovery is applicable to any fixed wing aircraft, including a transport aircraft with a very limited flight envelope (2.5g manoeuvres in pitch and about 30deg/sec roll rates). This is the main result of the paper. Therefore, the actual level of aircraft performance is not relevant for the ALSR algorithm. We have shown that the algorithm has a basis in the phugoid dynamics[9] and works to prevent departure via loss of airspeed.

For this study, the aircraft simulation model used is the ADMIRE (Aero-Data Model In a Research Environment) whose data is available in the public domain[14]. It may be noted that the carefree handling capability for the angle of attack and load factor is also available for ADMIRE[15]. The baseline controller was tested by applying and holding the full back stick. The simulation result showed that this input resulted in a low-speed departure. For the same input, it was found that the ADMIRE model does not recover at high pitch attitudes with the USAF aircraft recovery technique. In contrast, the Eurofighter ALSR[13], is expected to achieve successful recovery. In comparison to the ALSR-FP, the Eurofighter ALSR approach is considered more complex as it uses more parameters for decision like γ, Vdot, γdot, mass, throttle, configurations. Furthermore, we show how our proposed ALSR-FP algorithm can be adapted with minimal efforts to the other aircraft platforms.

The paper is organized as: Section 2 presents the details of the ADMIRE model. Section 3 presents the design of the proposed Auto Low Speed Recovery (ALSR-FP) algorithm for protection against the low-speed departure by relating it to the Phugoid motion. Section 4 presents the results and discussions of the Auto Low Speed Recovery (ALSR-FP) algorithm for various pilot input conditions and Mach numbers. A comparative study is presented in Section 5 to bring out the uniqueness and effectiveness of ALSR-FP over existing ALSR techniques on other aircraft programs that are available in the open literature. Finally, Section 6 summarizes the conclusions from this study.

2. ADMIRE AIRCRAFT SIMULATION MODEL

The aircraft simulation model used for the present study is the Aero-Data Model In a Research Environment (ADMIRE) model[14]. ADMIRE is a nonlinear, 6-DoF simulation model developed by the Swedish Aeronautical Research Institute using the aero data of a generic single seater, single engine fighter aircraft with a delta-canard configuration. This single seat fighter aircraft has multiple pairs of control surfaces. On the wing leading edge, it has flaps on either side. The control surfaces used for the pitch and roll control are called as Elevons and are located at the trailing edge of the wing in pairs (inboard and outboard). The forward located canards are all moving type. These control surface pairs can be used together or in a differential mode. The aircraft also has a vertical tail with Rudder (Fig. 3). These surfaces are used primarily as moment creating devices. The aircraft is equipped with the pitch and yaw control thrust vectoring nozzles.

The augmented ADMIRE 6-DoF Simulink model is available with the scheduled gain controller over the entire flight envelope to ensure the robust stability and handling performance[14]. The model also contains saturation and rate
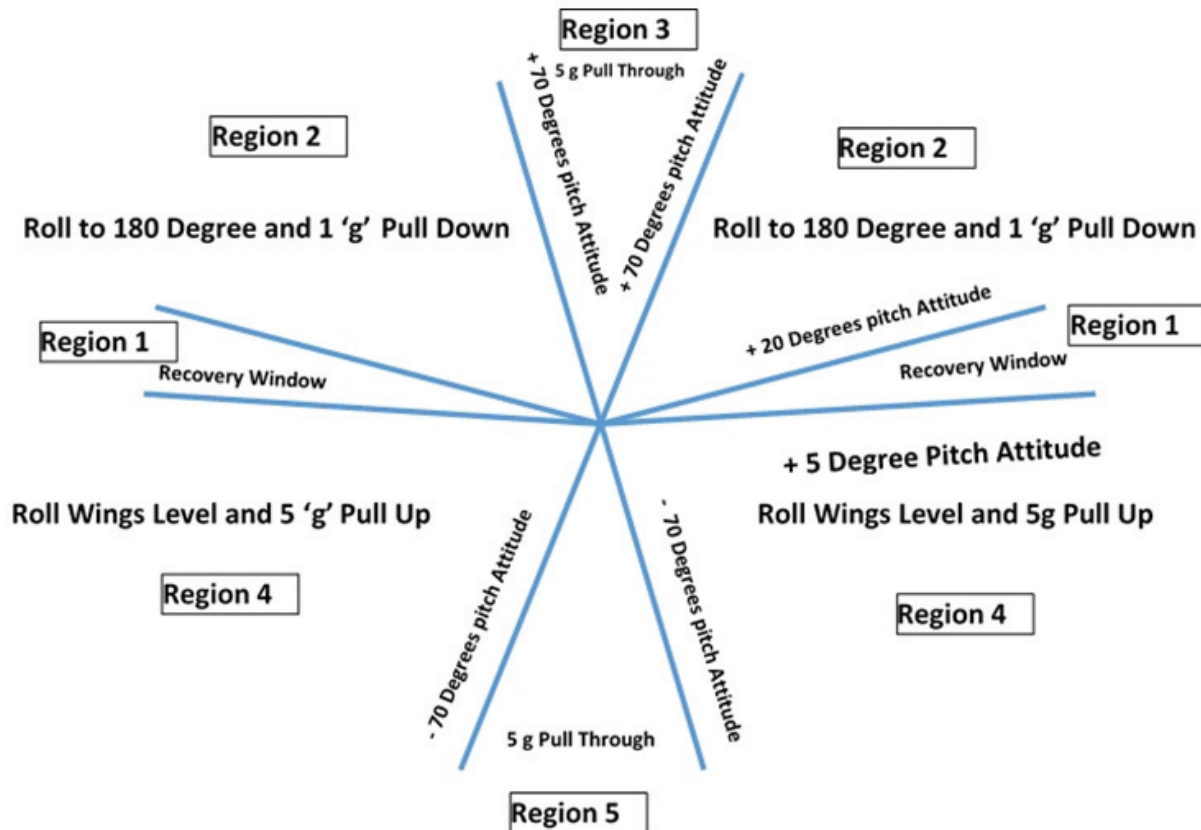

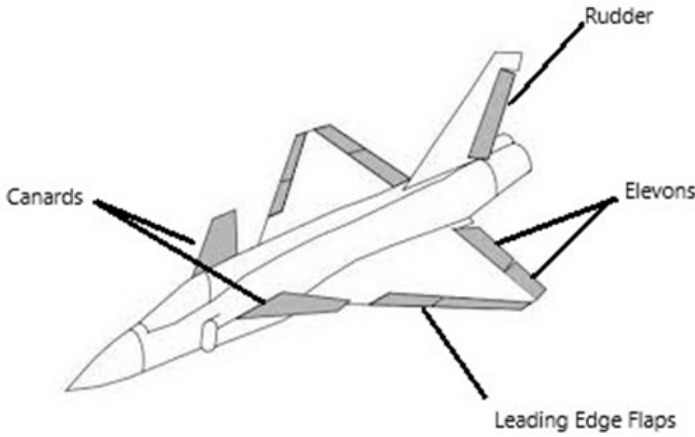**Figure 2. Pilot activated recovery regions[10].**

Figure 3. ADMIRE configuration.

limiting blocks along with a nonlinear stick shaping component in the forward path. The controller design has the variables α, β for feedback as the outer loop and pitch rate, stability axis roll rate and yaw rate as the inner loop feedback parameters. The ADMIRE model also includes the engine dynamics and detailed nonlinear actuator models[14].

From the initial simulation results (as presented in the next section), it is seen that though the ADMIRE model with q- Nz demand controller in the longitudinal axis has an 'α' protection feature, it does not provide adequate protection at high 'α' (>23º). The basic longitudinal FCS of the ADMIRE is designed for a trim angle of attack below 20.5 deg corresponding to Mach 0.2 at 6000 m. The following modifications in the ADMIRE model have been incorporated by us in order to avoid short term departure due to exceeding the α:

• The maximum angle of attack is limited to 20º at low speeds

with a margin up to 23 degrees to allow for overshoots. The angle of attack limiting on both the positive upper limit and the negative lower limit is achieved by a one-sided feedback gain which acts on the negative error and positive error respectively.

• The max stick demand in the roll channel was originally scaled to 180 deg/sec irrespective of the Mach number. Below (about) 0.3 Mach, this has been reduced to 60º/sec to avoid actuator saturation. The above two modifications do not in any way reduce the performance at higher speeds. For example, the aircraft is able to achieve 8g manoeuvres as well as design roll rates at higher speeds as before.

• A 0.25 second command path filter deep inside the roll channel has been moved to the outside the roll command path. A similar command path filter of time constant 0.25 sec was added to the pitch path. When pitch stick is neutral, the roll stick authority is maximum. Roll stick authority is linearly reduced to 50 % of its maximum value when pitch stick is at its maximum deflection. This maintains the elevon deflections within limits as these surfaces are used for both pitch and roll control in together and differential mode, respectively. The command path schematic is shown in Fig. 4.

• Gravity compensation is carried out as per the design of SNDI controller in.[8]

All the simulation studies reported in this paper have been carried out with the updated ADMIRE model as described above. The simulation studies have been carried out in the Matlab & Simulink environment. The computer used for the purpose has an Intel core processor with the 4GB RAM, 2.13GHz processing speed and 512GB hard disk. In the next section, the proposed ALSR-FP algorithm is presented in detail.
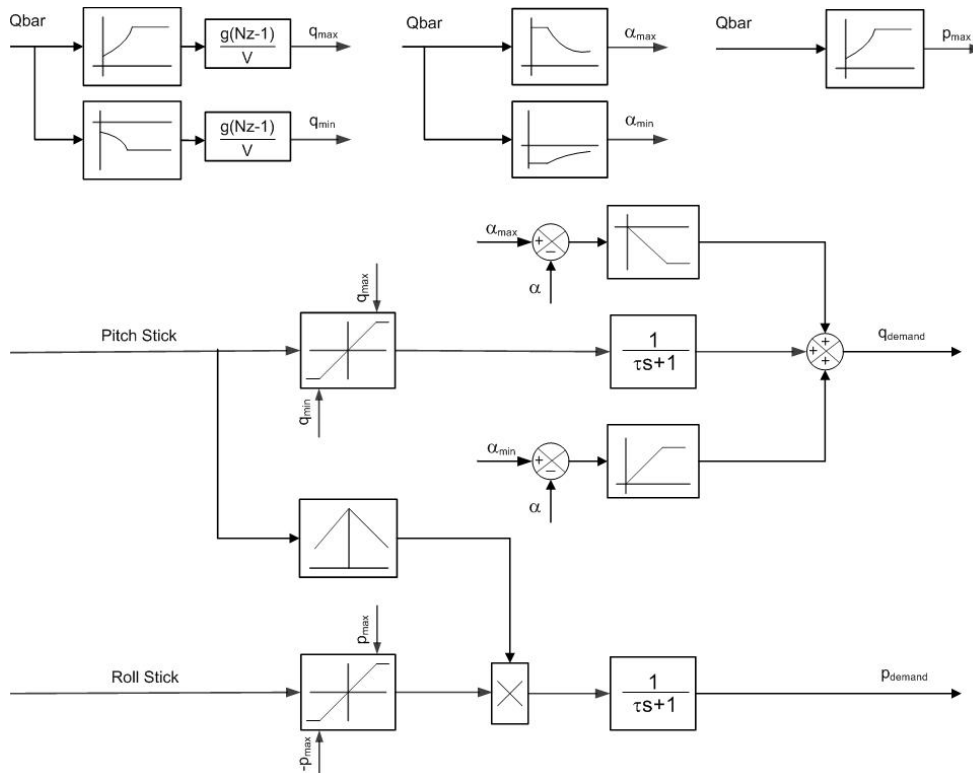

Figure 4. The command path implemented for ADMIRE.

3. DESIGN OF AUTOMATIC LOW SPEED RECOVERY - FORWARD PREDICTION (ALSR-FP) ALGORITHM

It may be noted that there could be many ways the pilot can enter into the low-speed region leading to the departure of the aircraft. One typical way to create such a condition is by starting from a straight level flight and pulling the pitch stick fully back. The aircraft response in Fig. 5 & Fig. 6 represents one such departure trajectory due to a pull up manoeuvre. In Fig. 5, the aircraft is seen flying in from South to North and commences a pull up after travelling 300 m North at an altitude of 5000 m. The aircraft thereafter, continues climbing to about 5600 m altitude. Each aircraft icon in this figure has been drawn at 5sec intervals, showing clearly the changes in the aircraft attitude and altitude.
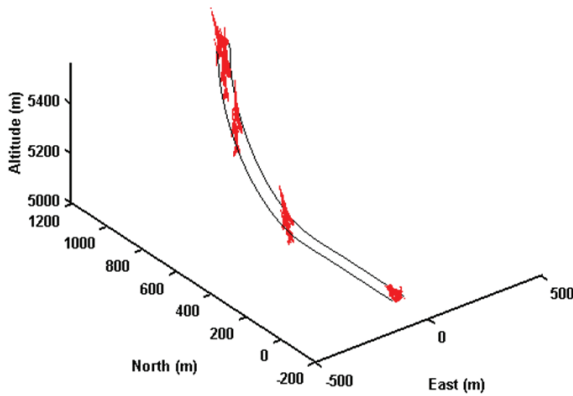

Figure 5. Pull Up from initial M=0.5, H=5000 m with baseline ADMIRE controller.

The aircraft response for the 3-D trajectory above is shown in Fig. 6. It is seen that when the full pitch back stick input is applied (at 2 s), elevon and rudder control surfaces saturate at 5 sec and 7 sec respectively as the airspeed falls below 92 Knots. In this simulation, the aircraft is initially flying at Mach 0.5 at an altitude of 5000 m. The 'α' continues to build up and reaches around 45⁰.

It may be noted that the manoeuvre simulated in Fig. 5 & Fig. 6, should result in the controller holding a constant angle of attack due to the limiters in the command path. Thus, during pull up manoeuvres, we are dealing with the phugoid mode of the aircraft, because in this mode, the aircraft velocity and the pitch angle participate and angle of attack is constant. The phase portrait (γ Vs non-dimensional speed) of the phugoid mode is analysed in the next section to obtain an insight into the nature of the dynamic behaviour of an aircraft. This also suggests a way to avoid departure due to loss of speed.

3.1 Mathematical Modelling of the Phugoid Motion

When the gravity vector is adverse (i.e., approximately opposite to the velocity vector) and the thrust is not adequate to oppose the drag, an aircraft will lose airspeed. The components of the gravity vector appear only in the translational equations of motion as given below:
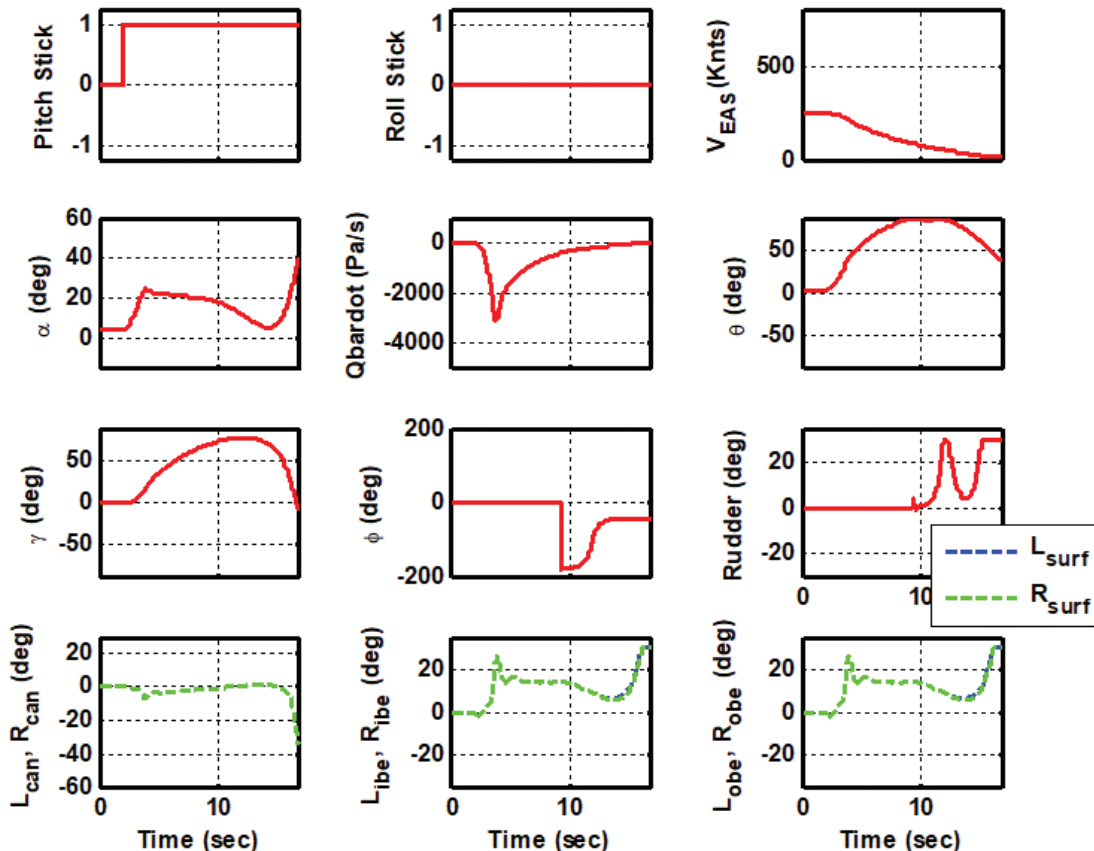
$$\dot{U} = R*V - Q*W - g*Sin\theta + \frac{T+Fx}{m}$$

Figure 6. Departure and loss of control with initial M=0.5, H=5000 m with baseline ADMIRE controller.

$$\dot{V} = -R*U - P*W - g*Sin\phi*Cos\theta + \frac{Fy}{m} \quad (1)$$

$$\dot{W} = Q*U - P*V - g*Cos\phi*Cos\theta + \frac{Fz}{m}$$

It is seen that if the wings are held level (i.e., bank angle $\phi = 0, \pi$), then the gravity component of the second of the three equations above vanishes. Further, as explained in the previous section, in a pull up manoeuvre, the angle of attack remains constant after it reaches the maximum limit. This means that the above equations representing the translational equations can be simplified to phugoid dynamics by considering motion in the vertical plane at a constant angle of attack:

$$\dot{V} = \frac{(T-D)}{m} - g*Sin\gamma$$

$$\dot{h} = V*Sin\gamma$$

$$\dot{\gamma} = \frac{(L - W*Cos\gamma)}{m*V} \quad (2)$$

By using suitable non-dimensional variables, the following systems of equation are obtained for phugoid motion. The resulting equations can be found in reference[9]:

$$\frac{dy}{d\tau} = b - a*y^2 - Sin\gamma \quad (3)$$

Where,

$$y = \frac{V}{V_0} \qquad a = \frac{C_D}{C_L} \qquad b = \frac{\tau}{m*g} \qquad \tau = \frac{g}{V_0}*t$$

$$V_0 = \sqrt{\frac{2*m*g}{\rho*S*C_L}} \quad (4)$$

For a typical case of an initial Mach number of 0.5, altitude of 5000m ($a=0.0929$, $b=0.0655$), the stability of the above system of equations is seen from the phase plane plot in Fig. 7. The trajectory has been generated for initial values of y in the range 0 to 3 and γ in the range -180⁰ to +180⁰. The arrows on each curve show the direction of the vector field. The point (0,1) represents the stable equilibrium point i.e. flight path angle, γ=0 and $V=V_0$ (1 'g' Trim velocity). The blackcolour horizontal line represents the minimum velocity, Vmin=61m/s at 5000 m (dynamic pressure of 1370 Pascals equal to 92 Knots of Equivalent airspeed). Below this speed aerodynamic control surfaces lose their effectiveness so that it is not possible to maintain the 'α'.

The solid green colour lines represent the trajectories that converge to an equilibrium point without the low-speed limit violation. The solid red-colour trajectories have adequate energy to diverge to another equilibrium point. The green dashed line (convergent to (0,1) equilibrium point) and another red dashed line (diverging to another equilibrium) end up below Vmin in Fig. 7. The blue colour trajectory represents the tail slide case, where the initial velocity (V) is just sufficient to cause the

aircraft to simultaneously achieve a flight path angle of 90⁰ and a zero velocity. This curve divides the green colour trajectories that tend to converge to the equilibrium point and the red colour trajectories that diverge to another equilibrium point. In fact, all the trajectories which fall between the trajectories marked as '1' and '2' in Fig. 7 eventually show a reduction of speed below the minimum speed and lead to departure (i.e., 'α' divergence, position and rate saturation of control surfaces). This is due to loss of aerodynamic control effectiveness.

3.2 Development of an Algorithm to Predict the Approach of Low-Speed Departure

It is clear that when the aircraft is maintaining a high 'α' at low speeds, the drag also increases. The increased drag has the potential to further reduce speed and thereby cause the aircraft to cross the low-speed boundary and depart from a controlled flight. From Eqn. (2) one can see that when the thrust is less than drag, the aircraft velocity will decrease. If the situation persists (i.e., the thrust continues to be deficient or pilot does not compensate by increasing the engine power), the only way to prevent the decay of velocity is to orient the velocity vector towards the direction of gravity by making the flight path angle 'γ' negative. Therefore, it is proposed that as part of the automatic low speed recovery, first the 'α' is brought down to zero if the bank angle at the time the ALSR-FP is engaged is lower than or equal to 60⁰. This will help reduce the aircraft drag. In case the bank angle is more than 60⁰, the aircraft is driven to an inverted position (bank angle 180⁰) and pull up command is given for the pitch stick. This logic described above enables orienting the velocity vector towards the gravity vector. The time or flight condition at which the ALSR-FP mode is triggered will determine if the aircraft will regain airspeed and recover successfully. It is clear that this time must be chosen in advance of the time instant when the aircraft reaches its departure airspeed. The method of arriving at this appropriate time or trigger condition is discussed in detail below.

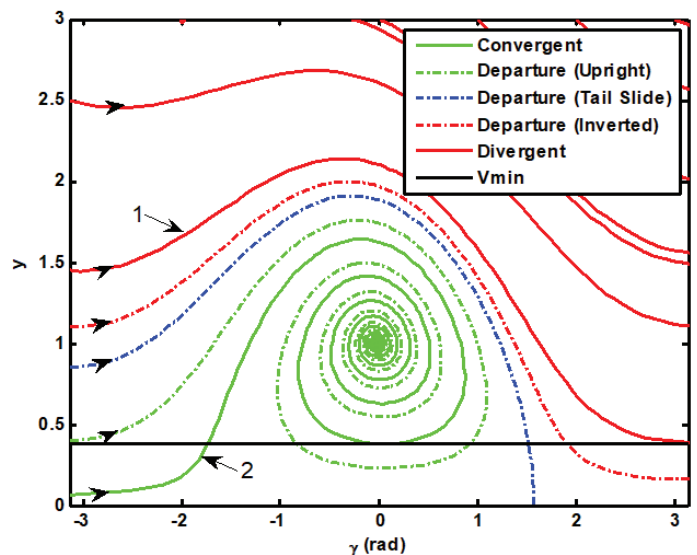The low-speed boundary of a typical fighter aircraft is a function of the maximum 'α' that it can sustain at a

Figure 7. Phase portrait of the phugoid with initial M=0.5, altitude 5000 m.

certain level flight condition (trim) and is therefore related to the dynamic pressure (Qbar). As a first step, the low-speed boundary for ADMIRE aircraft simulation model is worked out by conducting simulations of by holding full back stick pitch input at various starting Mach numbers at the altitude of 6000m (typical high altitude for ADMIRE). The simulation is conducted with the ADMIRE controller modified as explained in Section 2 to overcome the deficiencies in the angle of attack limiter of the baseline controller. The variation of Qbar and Qbardot has been plotted for different Mach numbers (0.3 to 0.828) and shown in Fig. 8 (Mach 0.828 simulation is shown in red colour). It is observed that for Mach≥0.828, no ALSR-FP trigger is needed as the aircraft has sufficient energy to complete the loop. The crossover points of the M=0.828 curve and the other Mach number curves are identified as the first cut estimates of the ALSR-FP trigger point. This will restrict the depletion of Qbar below the value defined by the red curve. The crossing points are separately shown in Fig. 9. It is interesting to note that this curve obtained by a series of simulations is nearly a straight line. It is seen in Fig. 8 and Fig. 9 that the Qbardot is zero at a value of Qbar of 1358 Pascals.

The Qbardot is negative due to the additional drag when the pitch stick is pulled fully back. Once the Qbardot falls below the trigger value (say "Qbardot_Limit") given by the plot in Fig. 9, the ALSR-FP is activated. This trigger boundary was tested by carrying out simulations for altitude variations from 1000m to 7000m (with the step size of 1000 m) and Mach variations from 0.45 to 0.85 with the step size of 0.05.

At any given altitude when the initial Mach number is high enough, the aircraft is able to complete the loop due to adequate kinetic energy. However, in some high Mach number cases the ALSR-FPis triggered when the pitch angle (theta) crossed 90⁰ and thetadot was negative. This was deemed undesirable and an additional condition of positive thetadot to trigger ALSR-FP is also introduced. The condition for the trigger of ALSR-FP is represented mathematically as given below in Eqn. (5).
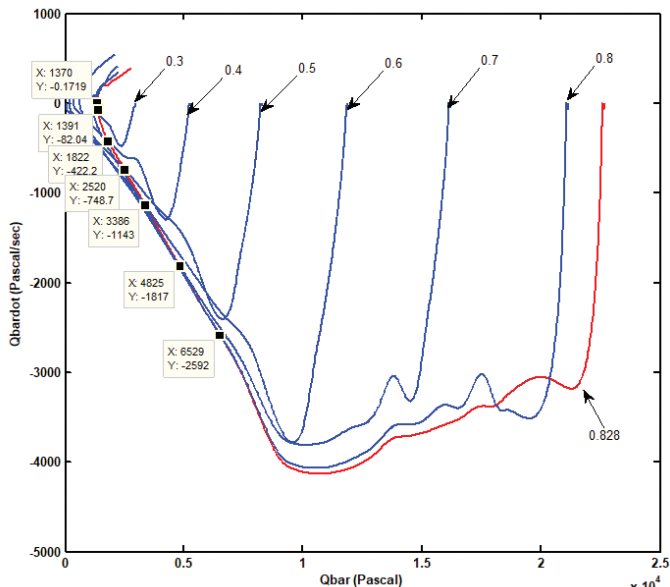

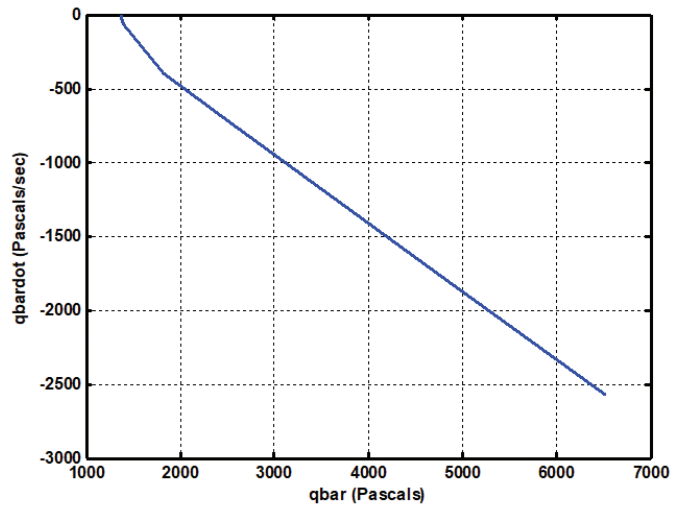**Figure 9. Trigger value of Qbar as a function of Qbardot.**

$$Qbar\_trigger = Current\_Qbardot < Qbardot\_Limit \&\& Thetadot > 0 \qquad (5)$$

If the values of the Qbar_trigger are expressed as a function of the Qbardot values and a straight line is fitted to this curve, the slope of this line has the units of a time constant, while the intercept is the value of Qbar at which Qbardot is zero (~1358 Pascal in this case). The time constant represents the time required to reach the intercept value of 1358 Pascal. Therefore, the proposed low speed recovery algorithm is called Automatic Low Speed Recovery with Forward Prediction (ALSR-FP) algorithm. The forward prediction time is found to be about 2 seconds.

Once the aircraft is put into the path of recovery, the process of alignment of velocity vector with the gravity vector begins and the speed and the dynamic pressure start increasing after an initial short period of decrease. It has been observed that the following logic is suitable for the handing over the controls back to the pilot.

$$Qbardot \geq 0 \text{ and } Qbar \geq 1520 \text{ Pascal} \qquad (6)$$

The higher value of 1520 Pascal has been chosen so that the automatic low speed recovery is not triggered again. Once the above condition is met, the ALSR-FP mode is reversed and the control stick authority is handed over back to the pilot. The pilot can then control the aircraft for the subsequent manoeuvres. In the aircraft, initiation of ALSR-FP and the completion of the recovery needs to be enunciated to the pilot appropriately.

Aircraft recovery based on this logic has been verified for various pilot input conditions like, holding Full back pitch stick, Full back stick input with aircraft holding a bank angle and capturing and holding different flight path angles. To summarise, the ALSR-FP algorithm can be developed for any high-performance fighter aircraft by following the step-by step approach given below:

- The 6-DoF simulation package with a valid Aero Data Set, Engine model, mass & CG data etc. Have to be used or if not available, needs to be developed.

Figure 8. Variation of Qbar as a function of Qbardot for different Mach number.

511

- A control law (base-line) has to be developed to achieve acceptable Handling and Flying qualities.
- The limiters for critical aircraft parameters like 'α' and Nz have to be incorporated and tested to verify that they work up to and above the minimum control airspeed needed.
- Simulations have to be carried out with a trim condition for a full back stick input at a higher altitude (say 6000m) to identify the Mach number at which the aircraft has sufficient energy to complete a loop starting from 1g wings level flight.
- At the same altitude, find the intersection of the simulation trajectory computed in the step above with similar trajectories computed by reducing the Mach number in steps of 0.1, in the Qbar vs Qbardot plane. Join the intersection points found between each of the latter trajectories with the trajectory computed in step above to obtain the trigger boundary for initiation of the low-speed recovery. This is the first phase, stated as low speed departure prediction.
- The automatic recovery mode consists of ignoring the pitch stick and roll stick and driving 'α' and bank angle to zero if the bank angle at the time of initiation is lower than 60⁰. In case the bank angle is more than 60⁰ when the recovery is triggered, the aircraft is driven to an inverted condition and simultaneously a pull down is performed. This second phase is the low speed departure recovery based on the aircraft conditions.
- Once the aircraft recovers to a sufficiently high dynamic pressure, the control is handed back to the pilot in the pitch and roll channels. This third phase is the final phase of ALSR to hand over the controls back to the pilot.
- Confirm the above trigger boundary and fine tune for other departure prone manoeuvres like bank and pull; 'γ' capture etc

Detailed simulation results highlighting the above are presented in the next Section.

4. RESULTS AND DISCUSSION

To successfully deploy the proposed ALSR-FP algorithm, it has to be tested for various carefree manoeuvring scenarios that will precipitate low-speed conditions. From previous work[1, 13, 16-21], and the experience in the flight testing of various fighter aircraft programs, it is seen that the low-speed conditions could occur during any of the following manoeuvres, viz., Air-to-Air tracking, capture tasks, Air to Ground Tracking and High 'α' aerobatic manoeuvres. Based on this, the following manoeuvres have been selected to achieve the low-speed condition:

- Pure pull-up manoeuvre - Pilot is concentrating on the aerobatic demonstration
- Pull-up with bank capture - Air to Air tracking tasks & Formation flights
- Flight path angle capture - Climb with a constant 'γ'

In reference 1, it is observed that the pilot disorientation recovery algorithm was demonstrated for different regions based on the aircraft pitch attitudes lying between -90⁰ to 90⁰. Here, the proposed ALSR-FP is tested for flight path angle in the range of 0 to 90⁰ and additionally for the bank angle in the positive range of 0 to 90⁰ (due to symmetry

considerations) for Mach numbers up to 0.85. Since the negative flight path angle aids recovery (due to assistance of gravity), a detailed analysis is carried out only for the positive flight path angles and the same are presented here. The above study covers the various aircraft manoeuvres of interest. In these simulations it is assumed that the throttle remains constant at its 1 'g' value. This is a conservative assumption for aircraft which do not have an auto-throttle.

For all the cases of Mach up to 0.85 and Altitude (1000 m to 7000m), the ALSR-FP shows a positive recovery whereas for many cases without this low-speed protection, it is seen that the aircraft departs from the controlled flight. The simulation result for one such case of pure Pull-up manoeuvre case is presented below.

An initial Mach number of 0.5 was chosen. The results of ALSR-FP simulation are given in Figs. 10, 11 and 12. Figure 10 shows the aircraft trajectory in three dimensions. The aircraft is trimmed at 5000 m and the full back stick input is applied at 2 s.This case is identical to Fig. 5 and Fig. 6 except that now the proposed ALSR-FP algorithm described (in the previous section) is active. The aircraft starts climbing and the low-speed recovery condition occurs and ALSR-FP is triggered. The aircraft nose down is applied for recovery. The original trajectory of departure without ALSR-FP is also plotted in red colour. It is seen that the red colour trajectory ends abruptly as in Fig. 5 due to the exceedance of aircraft parameters like, 'α', control surface position and rates. For this scenario, Fig. 11 shows the variations of aircraft parameters and control surface positions. The plots in blue and red colour represent the results of with and without ALSR-FP respectively. The control surface variation for ALSR-FP is in solid blue and green. Dashed blue and green colour curves show the saturation of rudder and elevon in the absence of the ALSR-FP. The red colour curve of 'α', rudder, bank angle and speed show a clear exceedance of parameters without ALSR-FP. In Fig. 11, the qbardot limit to trigger the ALSR-FP is plotted in dashed black colour.

It is seen from the same plot that the qbardot exceeds the qbardot trigger at 5.65 s and the ALSR-FP trigger is activated (shown as dashed black line in the plot of pitch and roll stick). The pilot control is disconnected and the ALSR-FP pitch stick forward input is generated. Since the bank angle is closer to zero, no roll command is generated. The recovery condition is met at around 17.5 s, ALSR-FP trigger=0. Thus, the aircraft recovers successfully and full control is handed over to the pilot.
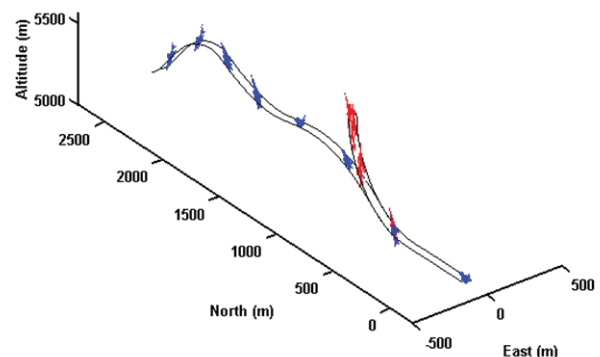

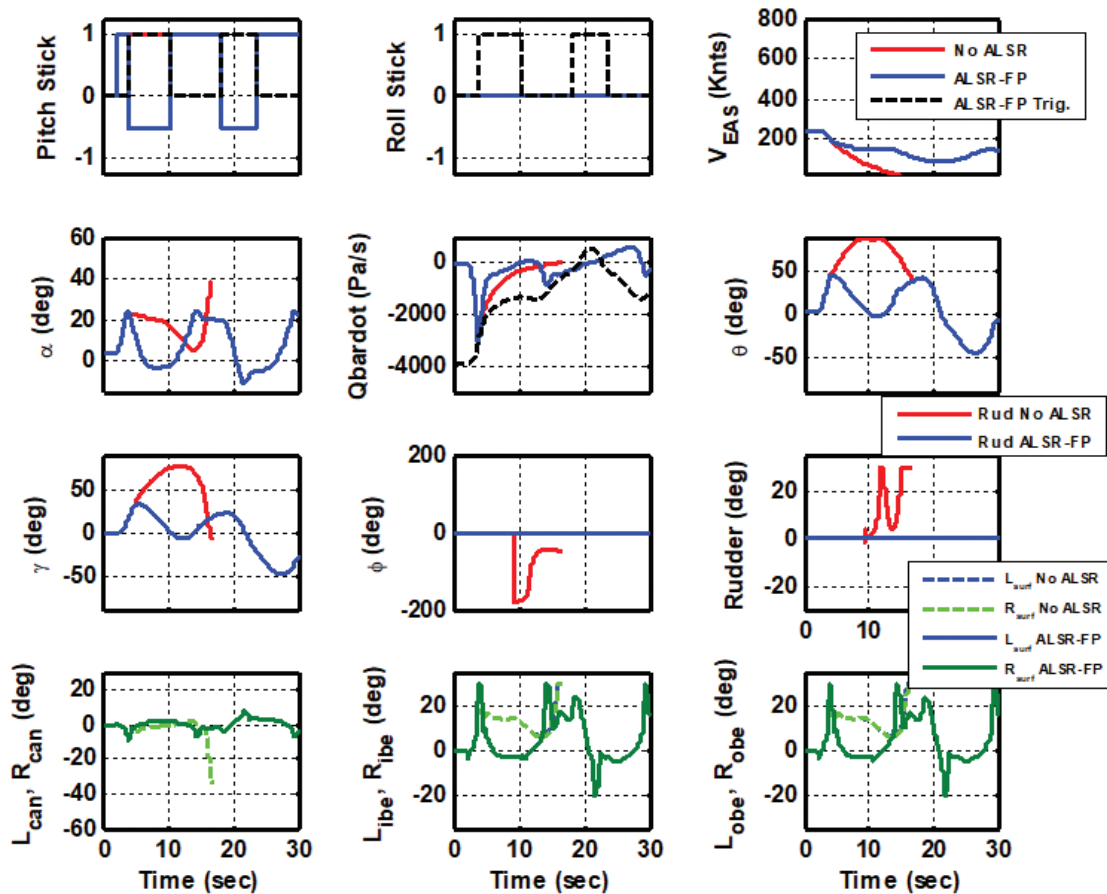**Figure 10. Aircraft Trajectory with initial M=0.5, H=5000m with and without ALSR-FP.**

Figure 11. Aircraft response with the initial M=0.5, H=5000 m with and without ALSR-FP.

Figure 12 presents the phase portrait variation of V/V_0 and the flight path angle 'γ'. It is clearly seen that the aircraft response with ALSR-FP (blue curve) shows a proactive initiation of recovery action and successful recovery of the aircraft and departure of the aircraft without ALSR-FP (red colour curve).

The study has been carried out for the other manoeuvres like pull-up with bank capture and flight path angle capture for a range of Mach numbers from 0.3 to 0.9 and Altitude=1000 m to 7000 m.It is found that the Auto recovery is successful for all the cases. This technique can be applied to indigenous fighter aircraft projects of the country.
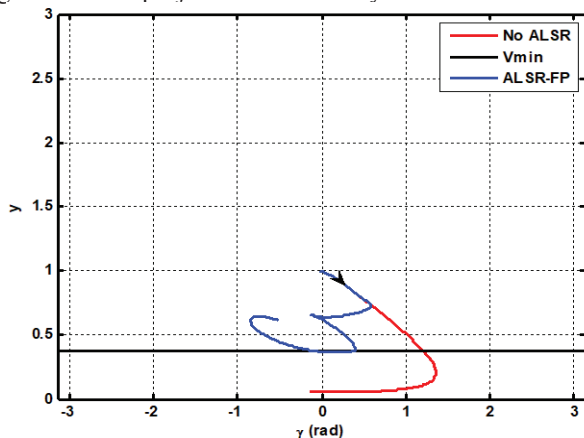

Figure 12. Variation γ and V/V_0 with initial M=0.5 with ALSR-FP.

5. COMPARISON WITH OTHER ALSR TECHNIQUES

The existing low-speed recovery techniques considered for comparison are Pilot Activated Recovery System (PARS) for a highly modified single seater fighter aircraft of USAF and the ALSR developed for the Eurofighter aircraft. For USAF aircraft, the recovery manoeuvre followed with different attitude of aircraft is given in Fig. 2[10]. It is seen that at moderate pitch attitude (Region 2: 20 to 70°), the recovery is by inverted pull-down. At high pitch attitudes (Region 3: > 70°), the recovery is by 5 'g' pull through.

When we compare with the PARS system in USAF fighter aircraft which is a pilot activated recovery technique the ALSR-FP is fully automatic. For the comparison of ALSR techniques, the study has been carried out for the region of high aircraft attitudes (θ>70°). From Fig. 10, Fig. 11 and Fig. 12, it is seen that the θ=70° occurred at around 5 sec. As per the USAF fighter aircraft recovery manoeuvre of 5 'g' pull through is similar to holding the full stick back. The simulation results given in Fig. 5 & Fig. 6 corresponds to the recovery manoeuvre of 5 'g' pull through (holding the stick fully back) assuming the throttle is constant at trim. The aircraft is departing due to the exceedance of 'α', surface positions etc. Airspeed at which the aircraft is able to generate 5 'g' is much higher than those at which ALSR-FP is shown to have a successful recovery. It shows that the PARS low-speed recovery technique is not suitable at extreme attitudes.

513

In case of the Eurofighter ALSR technique beyond flight path angle of 70⁰, it is recommended to invert the aircraft and pull the pitch stick fully back[13] to affect a recovery. It is not clearly specified when this action has to be taken (i.e., the trigger to initiate recovery action). From Figs. 10, 11 and 12, it is clear that a delay in taking this action can result in departure of the aircraft.

To consider the effect of the adequate thrust, the ADMIRE simulation is repeated with auto-throttle ON for the full back stick input with and without ALSR-FP for the same initial condition of M=0.5 and H=5000 m. In this case the aircraft does not depart and completes the loop successfully with and without ALSR-FP. The variation of aircraft parameters is within the limits and identical for both the cases. Therefore, compared to USAF PARS and Eurofighter ALSR techniques, the ALSR-FP is found to protect the aircraft against the low-speed departure with or without auto-throttle.

6.   CONCLUSIONS

Due to the high workload on the pilot of a high-performance fighter aircraft, Automatic Low-Speed Recovery (ALSR) is a desirable feature. Any ALSR technique consists of three parts, namely a trigger condition for initiation of the recovery, automatic actions by the flight control system to recover the airspeed followed by release of the controls back to the pilot after a successful recovery.

A novel approach for the design of the low-speed recovery called the Automatic Low Speed Recovery – Forward Prediction (ALSR-FP) has been presented. This is shown to be effective for a variety of manoeuvres across the Mach number range from 0.3 to 0.9 at all altitudes from 1000 m till 7000 m based on the ADMIRE aircraft simulation model. It is shown that the low-speed recovery is related to the phugoid mode of the aircraft. The trigger for initiation of the ALSR-FP is derived from trajectory simulations of the phugoid mode for various Mach numbers. Automatic recovery is triggered only when the pitch attitude rate is positive and a specific boundary in the space spanning the dynamic pressure and its rate of change is crossed.

A systematic procedure to establish this boundary has been developed and can be adapted for any other high-performance fighter aircraft. The automatic recovery actions of the flight control laws in the ALSR-FP mode for the pitch and roll controls are guided by the need to align as quickly as possible to the gravity vector. The condition for restoring controls back to the pilot after successful recovery are based on reaching a dynamic pressure approximately 10% higher than the minimum control speed of the aircraft in air. ALSR-FP can be used to safely expand the flight envelope of developmental aircraft in a step-by-step manner.

After successful flight testing and certification, this feature will enable protection of the aircraft from low-speed departures in its full flight envelope. ALSR-FP appears to be simpler to implement compared to existing algorithms and can be retro-fitted on an existing full authority control law.

REFERENCES

1.   Abzug, M. & Larrabee, E. Airplane stability and control: A history of the technologies that made aviation possible. Ed. 2, Cambridge Aerospace Series, Cambridge University Press. 2002.
doi: 10.1017/CBO9780511607141.

2.   Alcorn, C.W.; Croom, M.A.; Francis, M.S. & Ross, H. The X-31 aircraft: Advances in aircraft agility and performance. *Progress Aerospa. Sci.*, August 1996, **32**(4), 377-413.

3.   Muir, Ewan. The garteur high incidence research model (HIRM) benchmark problem. *AIAA Inc.*, AIAA-98-4243.
doi: 10.2514/6.1998-4243.

4.   Lee, Myung Sup; Lee, Young-Ho & Lee, Ilwoo. T-50/A-50 high angle of attack characteristics. AIAA-2006-6153, *AIAA Atmospheric Flight Mechanics Conf. and Exhibit*, Keystone, Colorado, 21-24 Aug. 2006.
doi: 10.2514/6.2006-6153.

5.   Zagainov, G. High manoeuvrability, theory and practice. AIAA-93-4737, *AIAA Aircraft Design, Systems and Operations Meeting,* Monterey, CA, August 1-13, 1993.
doi: 10.2514/6.1993-4737.

6.   Thunberg, J. & Robinson, J.W.C. Block backstepping, NDI and related cascade designs for efficient development of nonlinear flight control laws. AIAA-2008-6960, *AIAA Guidance, Navigation and Control Conf. and Exhibit,* Honolulu, Hawai. 18-21 Aug. 2008.
doi: 10.2514/6.2008-6960.

7.   Knoos, J.; Robinson, J.W.C. & Berefelt, F. Nonlinear dynamic inversion and block back stepping: A comparison. AIAA-2012-4888, *AIAA Guidance, Navigation, and Control Conf.*, Minneapolis, Minnesota, 13-16 Aug. 2012.
doi: 10.2514/6.2012-4888.

8.   Lathasree, P.; Ismail, S. & Pashilkar, A.A. Design of nonlinear flight controller for fighter aircraft. Advances in Control and Optimization of Dynamical Systems Conference, IIT Kanpur, Kanpur, India, 2013.

9.   Goman, M.G.; Zagainov, G.I. and Khramtsovsky, A.V. Application of bifurcation methods to nonlinear flight dynamics problems. *Progress in Aerosp. Sci.*, 1997, **33**(9), 539-586.

10.   Moorhouse, David J. Flight control design – Best practices. RTO Technical Report 29, NATO Research and Technology Organisation, December 2000.

11.   Jebakumar, S.K.; Navendu, Kumar and Pashilkar, A.A. Flight envelope protection for a fighter aircraft. Sixth Indian Control Conference, IIT Hyderabad, India, 18–20 December, 2019.

12.   Jayalakshmi, M.; Patel, Vijay V. & Singh, Giresh K. Relook at aileronto rudder interconnect. *Def. Sci.J.*, 2021, **71**(2), 153-161.
doi:10.14429/dsj.71.15347.

13.   Bowman, M. & Bremridge, A. The automatic low speed recovery function for the eurofighter typhoon aircraft and how it was flight tested. Annual Symposium of the Society of Flight Test Engineers European Chapter, London, 2004.

14.   Forssell, Lars S; Hovmark, Gunnar; Hyden, Ake & Fredrik Johansson, The aero-data model in a research environment (ADMIRE) for flight control robustness

evaluation. GARTUER/TP-119-7, 1st August 2001.

15. Amato,F.; Matte1, M.; Scala, S. & Verde, L.. Robust flight control design for the hlrm via linear quadratic methods. *AIAA Inc*., AIAA-98-4244.
doi: 10.2514/6.1998-4244.

16. Huffman, R.E.; Skoog, M.A.; Pinerio, L. & Ferm, M. Application of ground collision avoidance system nuisance criteria. 21st Congress of the International Council of the Aeronautical Sciences, (ICAS 98), Melbourne, Australia, September 1998.

17. Mason, W.H. Randolph 331A, Lecture series on high angle of attack aerodynamics. http://www.dept.aoe.vt.edu/~mason/Mason_f/ConfigAeroHiAlphaNotes.pdf [Accessed on 19 March 2015].

18. Shin, Ho-Hyun; Lee, Sang-Hyun; Kim, You-Dan; Kim, Eung-Tae & Sung, Ki Jung. Design of a flight envelope protection system using a dynamic trim algorithm. *Int. J. Aeronaut. Space Sc.*, 2011, **12**(3), 241–251.

19. Fu, Junquan; Shi, Zhiwei; Gong, Zheng; Lowenberg, Mark H.; Wu, Dawei & Pan, Lijun. Virtual flight test techniques to predict a blended wing-body aircraft in-flight departure characteristics. *Chin. J. Aeronaut.*, 2022, **35**(1), 215–225.
doi: 10.1016/j.cja.2021.01.006.

20. Osterhuber, R. Realization of the eurofighter 2000 primary lateral/directional control laws with differential pi-algorithm. *AIAA Guidance, Navigation and Control Conf. 2004, Providence RI, Proc.* AIAA 2004-4751.
doi: 10.2514/6.2004-4751

21. Bowman, Mark. MRAES Typhoon Project Test Pilot-BAE SYSTEMS Alex Bremridge MEng, MSc Senior Flight Test Engineer - BAE SYSTEMS. The automatic low speed recovery function for the eurofighter typhoon aircraft and how it was flight tested., Society of experimental test pilots (SFTE) conference 2004

CONTRIBUTORS

Mr SK Jebakumar is currently working at the Centre for Military Airworthiness and Certification (CEMILAC), Bangaluru since March 1997. He has completed his BTech (Aeronautical Engineering) from Madras Institute of Technology, Chennai in 1995 and ME (Aerospace Engineering) from Indian Institute of Technology in the year 2003. He is involved in the Certification of Military Aircraft and Unmanned Aerial Vehicles, majorly in the area of Aerodynamic clearance of various configurations of air systems and CLAW/Auto pilot CLAW/ Air Data System Airworthiness Clearances. Currently, as the Group Director (Aircraft & UAV) in CEMILAC, he is looking after the airworthiness certification of various indigenous military aircraft and UAV programs.
In the current study, he carried out the development of initial concept, implementation and generation of results.

Dr Abhay Pashilkar is working with CSIR-NAL since 1993. He joined the Flight Mechanics & Control Division (FMCD), NAL in 1991 and subsequently completed his PhD in Aerospace Engineering from IISc in 2002. Currently, he is Head of the Systems Engineering Division at CSIR-NAL and is also the Program Director for civil aircraft projects at NAL. His areas of interest are: Modeling, simulation, control and parameter estimation of aerospace systems.
His contributions in the current study involve the initial concept, manuscript preparation and review.

Dr N. Sundararajan received BE in Electrical Engineering from the Alagappa Chettiar College of Engg. & Tech., Karaikudi, University of Madras in 1966, and PhD in Electrical Engineering from the University of Illinois, Urbana-Champaign in 1971. From 1972 to 1991, he worked in the Indian Space Research Organization, Trivandrum, India starting as a Control System Designer to Director, Launch Vehicle Design Group contributing to the design and development of the Indian satellite launch vehicles SLV3, ASLV, PSLV and GSLV. He worked as the Project Engineer (Mission) for the first Indian Satellite Launch Vehicle project SLV3 team working directly under Dr. Kalam. His research interests are in the areas of aerospace control, machine learning, neural networks and applications and computational intelligence and have more than 250 papers and also five books in the area of neural networks.
In the current study, he carried out the manuscript preparation and review.